Modeling functional enrichment improves polygenic prediction accuracy in UK Biobank and 23andMe data sets

Carla Márquez-Luna[1], Steven Gazal[2,3], Po-Ru Loh[3,4], Nicholas Furlotte[5], Adam Auton[5], 23andMe Research Team[5], Alkes L. Price[1,2,3]

[1]Department of Biostatistics, Harvard School of Public Health, Boston, MA, USA.

[2]Department of Epidemiology, Harvard T.H. Chan School of Public Health, Boston, MA, USA.

[3]Program in Medical and Population Genetics, Broad Institute of Harvard and MIT, Cambridge, MA, USA.

[4]Division of Genetics, Department of Medicine, Brigham and Women's Hospital and Harvard Medical School, Boston, Massachusetts, USA.

[5]23andMe Inc., Mountain View, CA, USA.

Abstract

Genetic variants in functional regions of the genome are enriched for complex trait heritability. Here, we introduce a new method for polygenic prediction, LDpred-funct, that leverages trait-specific functional enrichments to increase prediction accuracy. We fit priors using the recently developed baseline-LD model, which includes coding, conserved, regulatory and LD-related annotations. We analytically estimate posterior mean causal effect sizes and then use cross-validation to regularize these estimates, improving prediction accuracy for sparse architectures. LDpred-funct attained higher prediction accuracy than other polygenic prediction methods in simulations using real genotypes. We applied LDpred-funct to predict 16 highly heritable traits in the UK Biobank. We used association statistics from British-ancestry samples as training data (avg N=365K) and samples of other European ancestries as validation data (avg N=22K), to minimize confounding. LDpred-funct attained a +27% relative improvement in prediction accuracy (avg prediction R^2=0.173; highest R^2=0.417 for height) compared to existing methods that do not incorporate functional information, consistent with simulations. For height, meta-analyzing training data from UK Biobank and 23andMe cohorts (total N=1107K; higher heritability in UK Biobank cohort) increased prediction R^2 to 0.429. Our results show that modeling functional enrichment substantially improves polygenic prediction accuracy, bringing polygenic prediction of complex traits closer to clinical utility.

Introduction

Genetic variants in functional regions of the genome are enriched for complex trait heritability [1–6]. In this study, we aim to leverage functional enrichment to improve polygenic prediction [7]. Several studies have shown that incorporating prior distributions on causal effect sizes can improve prediction accuracy [8–11], compared to standard Best Linear Unbiased Prediction (BLUP) or Pruning+Thresholding methods [12–14]. Recent efforts to incorporate functional information have produced promising results [15,16], but may be limited by dichotomizing between functional and non-functional variants [15] or restricting their analyses to genotyped variants [16].

Here, we introduce a new method, LDpred-funct, for leveraging trait-specific functional enrichments to increase polygenic prediction accuracy. We fit functional priors using our recently developed baseline-LD model [17], which includes coding, conserved, regulatory and LD-related annotations. LDpred-funct first analytically estimates posterior mean causal effect sizes, accounting for functional priors and LD between variants. LDpred-funct then uses cross-validation within validation samples to regularize causal effect size estimates in bins of different magnitude, improving prediction accuracy for sparse architectures. We show that LDpred-funct attains higher polygenic prediction accuracy than other methods in simulations with real genotypes, analyses of 16 highly heritable UK Biobank traits, and meta-analyses of height using training data from UK Biobank and 23andMe cohorts.

Material and Methods

Polygenic prediction methods

We compared 5 main prediction methods: Pruning+Thresholding [13,14] (P+T), LDpred-inf [11], P+T with functionally informed LASSO shrinkage [15] (P+T-funct-LASSO), and our new the LDpred-funct-inf method, and our new LDpred-funct method. P+T and LDpred-inf are polygenic prediction methods that do not use functional annotations. P+T-funct-LASSO is a modification of P+T that corrects marginal effect sizes for winner's curse, accounting for functional annotations. LDpred-funct-inf is an improvement of LDpred-inf that incorporates functionally informed priors on causal effect sizes. LDpred-funct is an improvement of LDpred-funct-inf that uses cross-validation to regularize posterior mean causal effect size estimates, improving prediction accuracy for sparse architectures. Each method is described in greater detail below. In both simulations and analyses of real traits, we used squared correlation (R^2) between predicted phenotype and true phenotype in a held-out set of samples as our primary measure of prediction accuracy.

P+T. The P+T method builds a polygenic risk score (PRS) using a subset of independent SNPs obtained via informed LD-pruning [14] (also known as LD-clumping) followed by P-value thresholding [13].

Specifically, the method has two parameters, R^2_{LD} and P_T, and proceeds as follows. First, the method prunes SNPs based on a pairwise threshold R^2_{LD}, removing the less significant SNP in each pair. Second, the method restricts to SNPs with an association P-value below the significance threshold P_T. Letting M be the number of SNPs remaining after LD-clumping, polygenic risk scores (PRS) are computed as

$$PRS(P_T) = \sum_{i=1}^{M} \mathbb{1}_{\{P_i < P_T\}} \tilde{\beta}_i g_i, \tag{1}$$

where $\tilde{\beta}_i$ are normalized marginal effect size estimates and g_i is a vector of normalized genotypes for SNP i. The parameters R^2_{LD} and P_T are commonly tuned using validation data to optimize prediction accuracy [13,14]. While in theory this procedure is susceptible to overfitting, in practice, validation sample sizes are typically large, and R^2_{LD} and P_T are selected from a small discrete set of parameter choices, so that overfitting is considered to have a negligible effect [13,14,18,19]. Accordingly, in this work, we consider $R^2_{LD} \in \{0.1, 0.2, 0.5, 0.8\}$ and $P_T \in \{1, 0.3, 0.1, 0.03, 0.01, 0.003, 0.001, 3*10^{-4}, 10^{-4}, 3*10^{-5}, 10^{-5}, 10^{-6}, 10^{-7}, 10^{-8}\}$, and we always report results corresponding to the best choices of these parameters. The P+T method is implemented in the PLINK software (see Web Resources).

LDpred-inf. The LDpred-inf method estimates posterior mean causal effect sizes under an infinitesimal model, accounting for LD [11]. The infinitesimal model assumes that normalized causal effect sizes have prior distribution $\beta_i \sim N(0, \sigma^2)$, where $\sigma^2 = h^2_g/M$, h^2_g is the SNP-heritability, and M is the number of SNPs. The posterior mean causal effect sizes are

$$E(\boldsymbol{\beta}|\tilde{\boldsymbol{\beta}}, \mathbf{D}) = (\frac{N}{1-h^2_l} * \mathbf{D} + \frac{1}{\sigma^2}\mathbf{I})^{-1} N * \tilde{\boldsymbol{\beta}}, \tag{2}$$

where $\mathbf{D}$ is the LD matrix between markers, $\mathbf{I}$ is the identity matrix, N is the training sample size, $\tilde{\boldsymbol{\beta}}$ is the vector of marginal association statistics, and $h^2_l \approx kh^2/M$ is the heritability of the k SNPs in the region of LD; following ref. 11 we use the approximation $1 - h^2_l \approx 1$, which is appropriate when $M >> k$. $\mathbf{D}$ is typically estimated using validation data, restricting to non-overlapping LD windows. We determined that an LD window size corresponding to approximately 0.15% of all (genotyped and imputed) SNPs is sufficiently large in practice. h^2_g can be estimated from raw genotype/phenotype data [20,21] (the approach that we use here; see below), or can be estimated from summary statistics using the aggregate estimator as described in ref. 11. To approximate the normalized marginal effect size ref. 11 uses the p-values to obtain absolute Z scores and then multiplies absolute Z scores by the sign of the estimated effect size. When sample sizes are very large, p-values may be rounded to zero, in which case we approximate normalized marginal effect sizes $\widehat{\beta}_i$ by $\widehat{b}_i \frac{\sqrt{2*p_i*(1-p_i)}}{\sqrt{\sigma^2_Y}}$, where $\widehat{b}_i$ is the per-allele marginal effect size estimate, p_i is the minor allele frequency of SNP i, and σ^2_Y is the phenotypic variance in the training data. This applies to all the methods that use normalized effect

sizes.

Although the published version of LDpred-inf requires a matrix inversion (Equation 2), we have implemented a computational speedup that computes the posterior mean causal effect sizes by efficiently solving[22] the system of linear equations $(\frac{1}{\sigma^2}\mathbf{I} + N * \mathbf{D})E(\boldsymbol{\beta}|\tilde{\boldsymbol{\beta}}, \mathbf{D}) = N\tilde{\boldsymbol{\beta}}$.

LDpred[11] is an extension of LDpred-inf that uses a point-normal prior to estimate posterior mean effect sizes via Markov Chain Monte Carlo (MCMC). In this work, we do not include LDpred in our main analyses; we determined in our secondary analyses that LDpred performs worse than LDpred-inf when applied to the UK Biobank data set that we analyze here (see Results).

P+T-funct-LASSO. Ref. 15 proposed an extension of P+T that corrects the marginal effect sizes of SNPs for winner's curse and incorporates external functional annotation data (P+T-funct-LASSO). The winner's curse correction is performed by applying a LASSO shrinkage to the marginal association statistics of the PRS:

$$PRS_{LASSO}(P_T) = \sum_{i=1}^{M} sign(\tilde{\beta}_i)||\tilde{\beta}_i| - \lambda(P_T)|\mathbb{1}_{\{P_i<P_T\}}g_i, \tag{3}$$

where $\lambda(P_T) = \Phi^{-1}(1 - \frac{P_T}{2})sd(\tilde{\beta}_i)$, where Φ^{-1} is the inverse standard normal CDF.

Functional annotations are incorporated via two disjoint SNPs sets, representing "high-prior" SNPs (HP) and "low-prior" SNPs (LP), respectively. We define the HP SNP set for P+T-funct-LASSO as the set of SNPs in the top 10% of expected per-SNP heritability under the baseline-LD model[17], the baseline-LD model includes coding, conserved, regulatory and LD-related annotations, whose enrichments are jointly estimated using stratified LD score regression[5,17] (see Baseline-LD model annotations section). We also performed secondary analyses using the top 5% (P+T-funct-LASSO-top5%). We define $PRS_{LASSO,HP}(P_{HP})$ to be the PRS restricted to the HP SNP set, and $PRS_{LASSO,LP}(P_{LP})$ to be the PRS restricted to the LP SNP set, where P_{HP} and P_{LP} are the optimal significance thresholds for the HP and LP SNP sets, respectively. We define $PRS_{LASSO}(P_{HP}, P_{LP}) = PRS_{LASSO,HP}(P_{HP}) + PRS_{LASSO,LP}(P_{LP})$. We also performed secondary analyses were we allow an additional regularization to the two PRS, that is: $PRS_{LASSO}(P_{HP}, P_{LP}) = \alpha_1 PRS_{LASSO,HP}(P_{HP}) + \alpha_2 PRS_{LASSO,LP}(P_{LP})$, we refer to this method as P+T-funct-LASSO-weighted.

LDpred-funct-inf. We modify LDpred-inf to incorporate functionally informed priors on causal effect sizes using the baseline-LD model[17], which includes coding, conserved, regulatory and LD-related annotations, whose enrichments are jointly estimated using stratified LD score regression[5,17]. Specifically, we assume that normalized causal effect sizes have prior distribution $\beta_i \sim N(0, c * \sigma_i^2)$, where σ_i^2 is the expected per-SNP heritability under the baseline-LD model (fit using training data

only) and c is a normalizing constant such that $\sum_{i=1}^{M} \mathbb{1}_{\{\sigma_i^2>0\}} c\sigma_i^2 = h_g^2$; SNPs with $\sigma_i^2 \leq 0$ are removed, which is equivalent to setting $\sigma_i^2 = 0$. The posterior mean causal effect sizes are

$$E[\boldsymbol{\beta}|\tilde{\boldsymbol{\beta}}, \mathbf{D}, \sigma_1^2, \ldots, \sigma_{M_+}^2] = \mathbf{W}^{-1} N * \tilde{\boldsymbol{\beta}} = \left[N * \mathbf{D} + \frac{1}{c} \begin{pmatrix} \frac{1}{\sigma_1^2} & \ldots & 0 \\ \vdots & \ddots & \vdots \\ 0 & \ldots & \frac{1}{\sigma_{M_+}^2} \end{pmatrix} \right]^{-1} N * \tilde{\boldsymbol{\beta}}, \quad (4)$$

where M_+ is the number of SNPs with $\sigma_i^2 > 0$.

The posterior mean causal effect sizes are computed by solving the system of linear equations $\mathbf{W} E[\boldsymbol{\beta}|\tilde{\boldsymbol{\beta}}, \mathbf{D}, \sigma_1^2, \ldots, \sigma_M^2] = N * \tilde{\boldsymbol{\beta}}$. h_g^2 is estimated as described above (see LDpred-inf). $\mathbf{D}$ is estimated using validation data, restricting to windows of size $0.15\% M_+$.

LDpred-funct. We modify LDpred-funct-inf to regularize posterior mean causal effect sizes using cross-validation. We partition the posterior mean causal effect sizes into K bins (similar to reference 23), where each bin has roughly the same sum of squared posterior mean effect sizes. Let $S = \sum_i E[\beta_i|\tilde{\beta}_i]^2$. To define each bin, we first rank the posterior mean effect sizes based on their squared values $E[\beta_i|\tilde{\beta}_i]^2$. We define bin b_1 as the smallest set of top SNPs with $\sum_{i \in b_1} E[\beta_i|\tilde{\beta}_i]^2 \geq \frac{S}{K}$, and iteratively define bin b_k as the smallest set of additional top SNPs with $\sum_{i \in b_1, \ldots, b_k} E[\beta_i|\tilde{\beta}_i]^2 \geq \frac{kS}{K}$. Let $PRS(k) = \sum_{i \in b_k} E[\beta_i|\tilde{\beta}_i] g_i$. We define

$$PRS_{LDpred-funct} = \sum_{k=1}^{K} \alpha_k PRS(k), \quad (5)$$

where the bin-specific weights α_k are optimized using validation data via 10-fold cross-validation. For each held-out fold in turn, we estimate the weights α_k using the samples from the other nine folds and compute PRS on the held-out fold using these weights. We then compute the average prediction R^2 across the 10 held-out folds. We set the number of bins (K) to be between 1 and 100, such that the number of samples used to estimate the K weights in each fold is ~300 times larger than K:

$$K = \min(100, \lceil \frac{0.9N}{300} \rceil), \quad (6)$$

where N is the number of validation samples. Thus, if there are ~300 validation samples or fewer, LDpred-funct reduces to the LDpred-funct-inf method. In simulations, we set K to 20 (based on 8,441 validation samples; see below), approximately concordant with Equation 6.

Simulations

We simulated quantitative phenotypes using real genotypes from the UK Biobank interim release (see below). We used up to 50,000 unrelated British-ancestry samples as training samples, and 8,441 samples of other European ancestries as validation samples (see below). We made these choices to minimize confounding due to shared population stratification or cryptic relatedness between training and validation samples (which, if present, could overstate the prediction accuracy that could be obtained in independent samples[24]), while preserving a large number of training samples. We restricted our simulations to 459,284 imputed SNPs on chromosome 1 (see below), fixed the number of causal SNPs at 2,000 or 5,000 (we also performed secondary simulations with 1,000 or 10,000 causal variants), and fixed the SNP-heritability h_g^2 at 0.5. We sampled normalized causal effect sizes β_i for causal SNPs from a normal distribution with variance equal to $\frac{\sigma_i^2}{p}$, where p is the proportion of causal SNPs and σ_i^2 is the expected causal per-SNP heritability under the baseline-LD model[17], fit using stratified LD score regression (S-LDSC)[5,17] applied to height summary statistics computed from unrelated British-ancestry samples from the UK Biobank interim release (N=113,660). We computed per-allele effect sizes b_i as $b_i = \frac{\beta_i}{\sqrt{2p_i(1-p_i)}}$, where p_i is the minor allele frequency for SNP i estimated using the validation genotypes. We simulated phenotypes as $Y_j = \sum_i^M b_i g_{ij} + \epsilon_j$, where $\epsilon_j \sim N(0, 1 - h_g^2)$. We set the training sample size to either 10,000, 20,000 or 50,000. The motivation to perform simulations using one chromosome is to be able to extrapolate performance at larger sample sizes[11] according to the ratio N/M, where N is the training sample size. We compared each of the five methods described above. For LDpred-funct-inf and LDpred-funct, we set baseline-LD model parameters for each functional annotation equal to the baseline-LD model parameters used to generate the data, representing a best-case scenario for LDpred-funct-inf and LDpred-funct. For LDpred-funct, we report adjusted-R^2 defined as $R^2 - (1 - R^2)\frac{K}{N-K-1}$, with N is the number of validation samples and K the number of bins.

Full UK Biobank data set

The full UK Biobank data set includes 459,327 European-ancestry samples and ∼20 million imputed SNPs[25] (after filtering as in ref. 20, excluding indels and structural variants). We selected 16 UK Biobank traits with phenotyping rate > 80% (> 80% of females for age at menarche, > 80% of males for balding), SNP-heritability $h_g^2 > 0.2$, and low correlation between traits (as described in ref. 20). We restricted training samples to 409,728 British-ancestry samples[25], including related individuals (avg N=365K phenotyped training samples; see Table S1). As in our simulations, we computed association statistics from training samples using BOLT-LMM v2.3[20]. We have made these association statistics publicly available (see Web Resources). We restricted validation samples to 25,112 samples of non-British European ancestry, after removing validation samples that were related

(> 0.05) to training samples and/or other validation samples (avg N=22K phenotyped validation samples; see Table S1). As in our simulations, we made these choices to minimize confounding due to shared population stratification or cryptic relatedness between training and validation samples (which, if present, could overstate the prediction accuracy that could be obtained in independent samples [24]), while preserving a large number of training samples. We analyzed 6,334,603 genome-wide imputed SNPs, after removing SNPs with minor allele frequency $< 1\%$, removing SNPs with imputation accuracy < 0.9, and removing A/T and C/G SNPs to eliminate potential strand ambiguity. We used h_g^2 estimates from BOLT-LMM v2.3 [20] as input to LDpred-inf, LDpred-funct-inf and LDpred-funct.

UK Biobank interim release

The UK Biobank interim release includes 145,416 European-ancestry samples [26]. We used the UK Biobank interim release both in simulations using real genotypes, and in a subset of analyses of height phenotypes (to investigate how prediction accuracy varies with training sample size).

In our analyses of height phenotypes, we restricted training samples to 113,660 unrelated (≤ 0.05) British-ancestry samples for which height phenotypes were available. We computed association statistics by adjusting for 10 PCs [27], estimated using FastPCA [28] (see Web Resources). For consistency, we used the same set of 25,030 validation samples of non-British European ancestry with height phenotypes as defined above. We analyzed 5,957,957 genome-wide SNPs, after removing SNPs with minor allele frequency $< 1\%$, removing SNPs with imputation accuracy < 0.9, removing SNPs that were not present in the 23andMe height data set (see below), and removing A/T and C/G SNPs to eliminate potential strand ambiguity. We analyzed the same set of 5,957,957 SNPs both in the height meta-analysis of interim UK Biobank and 23andMe data sets and in the height meta-analysis of full UK Biobank and 23andMe data sets.

In our simulations, we restricted training samples to up to 50,000 of the 113,660 unrelated British-ancestry samples, and restricted validation samples to 8,441 samples of non-British European ancestry, after removing validation samples that were related (> 0.05) to training samples and/or other validation samples. We restricted the 5,957,957 genome-wide SNPs (see above) to chromosome 1, yielding 459,284 SNPs after QC.

23andMe height summary statistics

The 23andMe data set consists of summary statistics computed from 698,430 European-ancestry samples (23andMe customers who consented to participate in research) at 9,898,287 imputed SNPs, after removing SNPs with minor allele frequency $< 1\%$ and that passed QC filters (which include filters on imputation quality, avg.rsq< 0.5 or min.rsq< 0.3 in any imputation batch, and imputation batch effects). Analyses were restricted to the set of individuals with $> 97\%$ European ancestry,

as determined via an analysis of local ancestry[29]. Summary association statistics were computed using linear regression adjusting for age, gender, genotyping platform, and the top five principal components to account for residual population structure. The summary association statistics will be made available to qualified researchers (see Web Resources).

We analyzed 5,957,935 genome-wide SNPs, after removing SNPs with minor allele frequency $< 1\%$, removing SNPs with imputation accuracy < 0.9, removing SNPs that were not present in the full UK Biobank data set (see above), and removing A/T and C/G SNPs to eliminate potential strand ambiguity.

Meta-analysis of full UK Biobank and 23andMe height data sets

We meta-analyzed height summary statistics from the full UK Biobank and 23andMe data sets. We define

$$PRS_{meta} = \gamma_1 PRS_1 + \gamma_2 PRS_2, \tag{7}$$

where PRS_i is the PRS obtained using training data from cohort i. The PRS can be obtained using P+T, P+T-funct-LASSO, LDpred-inf or LDpred-funct. The meta-analysis weights γ_i can either be specified via fixed-effect meta-analysis (e.g. $\gamma_i = \frac{N_i}{\sum N_i}$) or optimized using validation data[30]. We use the latter approach, which can improve prediction accuracy (e.g. if the cohorts differ in their heritability as well as their sample size). In our primary analyses, we fit the weights γ_i in-sample and report prediction accuracy using adjusted R^2 to account for in-sample fitting[30]. We also report results using 10-fold cross-validation: for each held-out fold in turn, we estimate the weights γ_i using the other nine folds and compute PRS on the held-out fold using these weights. We then compute the average prediction R^2 across the 10 held-out folds.

When using LDpred-funct as the prediction method, we perform the meta-analysis as follows. First, we use LDpred-funct-inf to fit meta-analysis weights γ_i. Then, we use γ_i to compute (meta-analysis) weighted posterior mean causal effect sizes (PMCES) via $PMCES = \gamma_1 PMCES_1 + \gamma_2 PMCES_2$, which are binned into k bins. Then, we estimate bin-specific weights α_k (used to compute (meta-analysis + bin-specific) weighted posterior mean causal effect sizes $\sum_{k=1}^{K} \alpha_k PMCES(k)$) using validation data via 10-fold cross validation.

Baseline-LD model annotations.

The baseline-LD model contains a broad set of 75 functional annotations (including coding, conserved, regulatory and LD-related annotations), whose enrichments are jointly estimated using stratified LD score regression[5,17]. For each trait, we used the τ_c values estimated for that trait to compute σ_i^2, the

expected per-SNP heritability of SNP i under the baseline-LD model, as

$$\sigma_i^2 = \sum_c a_c(i)\tau_c, \tag{8}$$

where $a_c(i)$ is the value of annotation c at SNP i.

Joint effect sizes τ_c for each annotation c are estimated via

$$E[\chi_i^2] = N \sum_c \tau_c l(i,c) + 1, \tag{9}$$

where $l(i,c)$ is the LD score of SNP i with respect to annotation a_c and χ_i^2 is the chi-square statistic for SNP i. We note that τ_c quantifies effects that are unique to annotation c. In all analyses of real phenotypes, τ_c and σ_i^2 were estimated using training samples only.

In our primary analyses, we used 489 unrelated European samples from phase 3 of the 1000 Genomes Project[31] as the reference data set to compute LD scores, as in ref. 17.

To verify that our 1000 Genomes reference data set produces reliable LD estimates, we repeated our LDpred-funct analyses using S-LDSC with 3,567 unrelated individuals from UK10K[32] as the reference data set (as in ref. 33), ensuring a closer ancestry match with British-ancestry UK Biobank samples. We also repeated our LDpred-funct analyses using S-LDSC with the baseline-LD+LDAK model (instead of the baseline-LD model), with UK10K as the reference data set. The baseline-LD+LDAK model (introduced in ref. 33) consists of the baseline-LD model plus one additional continuous annotation constructed using LDAK weights[34], which has values $(p_j(1-p_j))^{1+\alpha} w_j$, where $\alpha = -0.25$, p_j is the allele frequency of SNP j, and w_j is the LDAK weight of SNP j computed using UK10K data.

Results

Simulations

We performed simulations using real genotypes from the UK Biobank interim release and simulated phenotypes (see Material and Methods). We simulated continuous phenotypes with SNP-heritability $h_g^2 = 0.5$, using 476,613 imputed SNPs from chromosome 1. We selected either 2,000 or 5,000 variants to be causal; we refer to these as "sparse" and "polygenic" architectures, respectively. We sampled normalized causal effect sizes from normal distributions with variances based on expected causal per-SNP heritabilities under the baseline-LD model[17], fit using stratified LD score regression (S-LDSC)[5,17] applied to height summary statistics from British-ancestry samples from the UK Biobank interim release. We randomly selected 10,000, 20,000 or 50,000 unrelated British-ancestry samples as

training samples, and we used 8,441 samples of non-British European ancestry as validation samples. By restricting simulations to chromosome 1 ($\approx$ 1/10 of SNPs), we can extrapolate results to larger sample sizes ($\approx$ 10x larger; see Application to 16 UK Biobank traits), analogous to previous work [11].

We compared prediction accuracies (R^2) for five main methods: P+T [13,14], LDpred-inf [11], P+T-funct-LASSO [15], LDpred-funct-inf and LDpred-funct (see Material and Methods). Results are reported in Figure 1, Figure S1, Table S2 and Table S3. Among methods that do not use functional information, the prediction accuracy of LDpred-inf was similar to P+T for the sparse architecture and superior to P+T for the polygenic architecture, consistent with previous work [11]. Incorporating functional information via LDpred-funct-inf produced a 13.6% (resp. 13.4%) relative improvement for the sparse (resp. polygenic) architecture, compared to LDpred-inf. Accounting for sparsity using LDpred-funct further improved prediction accuracy, particularly for the sparse architecture, resulting in a 24.8 % (resp. 18.8%) relative improvement, compared to LDpred-inf. LDpred-funct performed slightly better than P+T-funct-LASSO for the sparse architecture and much better than P+T-funct-LASSO for the polygenic architecture. The difference in prediction accuracy between LDpred-inf and each other method, as well as the difference in prediction accuracy between LDpred-funct and each other method, was statistically significant in most cases (see Table S3). Although LDpred-funct used K=20 posterior mean causal effect size bins to regularize effect sizes in our main simulations, results were not sensitive to this parameter (Table S4); K=50 bins consistently performed slightly better, but we did not optimize this parameter. Simulations with 1,000 or 10,000 causal variants generally recapitulated these findings, although P+T-funct-LASSO performed better than LDpred-funct for the extremely sparse architecture (Table S2).

Our simulations are supportive of the potential advantages of LDpred-funct-inf and LDpred-funct. However, we caution that all of our simulations use the same model (the baseline-LD model) to simulate phenotypes and to compute predictions. Thus, our simulations should be viewed as a best case scenario for LDpred-funct-inf and LDpred-funct; a more realistic assessment of the advantages of these methods can only be obtained by analyzing real traits.

Application to 16 UK Biobank traits

We applied P+T, LDpred-inf, P+T-funct-LASSO, LDpred-funct-inf and LDpred-funct to 16 UK Biobank traits. We selected the 16 traits based on phenotyping rate > 80%, SNP-heritability $h_g^2 > 0.2$, and low correlation between traits (as described in ref. 20). We analyzed training samples of British ancestry (avg N=365K; see Table S1) and validation samples of non-British European ancestry (avg N=22K). We included 6,334,603 imputed SNPs in our analyses (see Material and Methods). We computed summary statistics and h_g^2 estimates from training samples using BOLT-LMM v2.3 [20] (see Table S5). We estimated trait-specific functional enrichment parameters for the baseline-LD model [17]

by running S-LDSC[5,17] on these summary statistics.

Results are reported in Figure 2 and Table S6, Table S7 and Table S8. Among methods that do not use functional information, LDpred-inf outperformed P+T (average relative improvement: +4%), consistent with simulations under a polygenic architecture. We previously developed a different method, LDpred[11], which uses a point-normal prior to estimate posterior mean effect sizes via Markov Chain Monte Carlo (MCMC), but we determined that LDpred performs worse than LDpred-inf in UK Biobank data (Table S8).

Incorporating functional information via LDpred-funct-inf produced a +17% average relative improvement, consistent with simulations (relative improvements ranged from +6% for body mass index to +35% for tanning ability). Accounting for sparsity using LDpred-funct further improved prediction accuracy (avg prediction R^2=0.173; highest R^2=0.417 for height), resulting in a +27% average relative improvement compared to LDpred-inf, consistent with simulations under a polygenic architecture (relative improvements ranged from +5% for body mass index to +104% for tanning ability). LDpred-funct also performed substantially better than P+T-funct-LASSO (+18% average relative improvement), consistent with simulations under a polygenic architecture. Although LDpred-funct used an average of $K = 67$ posterior mean causal effect size bins to regularize effect sizes in these analyses (see Equation 6), results were not sensitive to this parameter (Table S9); K=100 bins consistently performed slightly better, but we did not optimize this parameter. In addition, although our main analyses involved very large validation sample sizes (up to 25,032; Table S1), which aids the regularization step of LDpred-funct, the bulk of the improvement of LDpred-funct vs. LDpred-funct-inf remained when restricting to smaller validation sample sizes (as low as 1,000; see Table S10). We also evaluated a modification of P+T-funct-LASSO in which different weights were allowed for the two predictors (P+T-funct-LASSO-weighted; see Material and Methods), but results were little changed +4% average relative improvement vs. P+T-funct-LASSO (see Table S8). Similar results were also obtained when defining the "high-prior" (HP) SNP set for P+T-funct-LASSO using the top 5% of SNPs with the highest per-SNP heritability, instead of the top 10% (see Table S8).

We performed several secondary analyses using LDpred-funct-inf. First, we determined that incorporating baseline-LD model functional enrichments that were meta-analyzed across traits (31 traits from ref. 17), instead of the trait-specific functional enrichments used in our primary analyses, slightly reduced prediction accuracy (Table S8). Second, we determined that using our previous baseline model[5], instead of the baseline-LD model[17], slightly reduced prediction accuracy (Table S8). Third, we determined that inferring functional enrichments using only the SNPs that passed QC filters and were used for prediction had no impact on prediction accuracy (Table S8). Fourth, we determined that using UK10K (instead of 1000 Genomes) as the LD reference panel had virtually no impact on prediction accuracy (Table S8). Additional secondary analyses are reported in the

Discussion section.

Application to height in meta-analysis of UK Biobank and 23andMe cohorts

We applied P+T, LDpred-inf, P+T-funct-LASSO, LDpred-funct-inf and LDpred-funct to predict height in a meta-analysis of UK Biobank and 23andMe cohorts (see Material and Methods). Training sample sizes were equal to 408,092 for UK Biobank and 698,430 for 23andMe, for a total of 1,106,522 training samples. For comparison purposes, we also computed predictions using the UK Biobank and 23andMe training data sets individually, as well as a training data set consisting of 113,660 British-ancestry samples from the UK Biobank interim release. (The analysis using the 408,092 UK Biobank training samples was nearly identical to the analysis of Figure 2, except that we used a different set of 5,957,935 SNPs, for consistency throughout this set of comparisons; see Material and Methods.) We used 25,030 UK Biobank samples of non-British European ancestry as validation samples in all analyses.

Results are reported in Figure 3 and Table S11. The relative improvements attained by LDpred-funct-inf and LDpred-funct were broadly similar across all four training data sets (also see Figure 2), implying that these improvements are not specific to the UK Biobank data set. Interestingly, compared to the full UK Biobank training data set (R^2=0.416 for LDpred-funct), prediction accuracies were only slightly higher for the meta-analysis training data set (R^2=0.429 for LDpred-funct), and were lower for the 23andMe training data set (R^2=0.343 for LDpred-funct), consistent with the $\approx 30\%$ higher heritability in UK Biobank as compared to 23andMe and other large cohorts [17,20,21]; the higher heritability in UK Biobank could potentially be explained by lower environmental heterogeneity. We note that in the meta-analysis, we optimized the meta-analysis weights using validation data (similar to ref. 30), instead of performing a fixed-effect meta-analysis. This approach accounts for differences in heritability as well as sample size, and attained a $> 3\%$ relative improvement compared to fixed-effects meta-analysis (see Table S11).

Discussion

We have shown that leveraging trait-specific functional enrichments inferred by S-LDSC with the baseline-LD model [17] substantially improves polygenic prediction accuracy. Across 16 UK Biobank traits, we attained a +17% average relative improvement using a method that leverages functional enrichment (LDpred-funct-inf) and a +27% average relative improvement using a method that performs an additional regularization step to account for sparsity (LDpred-funct), compared to the most accurate method tested that does not model functional enrichment (LDpred-inf).

Previous work has highlighted the potential advantages of leveraging functional enrichment to

improve prediction accuracy[15,16]. We included one such method[15] (which we call P+T-funct-LASSO) in our analyses, determining that LDpred-funct attains a +18% average relative improvement vs. P+T-funct-LASSO across 16 UK Biobank traits. Another method of interest is the AnnoPred method of ref. 16, which is closely related to LDpred-funct-inf. However, ref. 16 considers only genotyped variants and binary annotations. We determined that functional enrichment information is far less useful when restricting to genotyped variants (+1% improvement for LDpred-funct-inf (typed) vs. LDpred-inf (typed); Table S8), likely because tagging variants may not belong to enriched functional annotations; also, as noted above, the additional regularization step of LDpred-funct substantially improves prediction accuracy.

Our work has several limitations. First, LDpred-funct analyzes summary statistic training data (which are publicly available for a broad set of diseases and traits[35]), but methods that use raw genotypes/phenotypes as training data have the potential to attain higher accuracy[20]; incorporating functional enrichment information into prediction methods that use raw genotypes/phenotypes as training data remains a direction for future research. Second, the regularization step employed by LDpred-funct to account for sparsity relies on heuristic cross-validation instead of inferring posterior mean causal effect sizes under a prior sparse functional model; we made this choice because the appropriate choice of sparse functional model is unclear, and because inference of posterior means via MCMC may be subject to convergence issues. As a consequence, the improvement of LDpred-funct over LDpred-funct-inf is contingent on the number of validation samples available for cross-validation; in particular, for small validation samples, the number of cross-validation bins is equal to 1 (Equation 6) and LDpred-funct is identical to LDpred-funct-inf. Third, we have considered only single-trait analyses, although leveraging genetic correlations among traits has considerable potential to improve prediction accuracy[36,37]. Fourth, we have not considered how to leverage functional enrichment for polygenic prediction in related individuals[38]. Fifth, we have not investigated the application of our methods to polygenic prediction in diverse populations[30], for which very similar functional enrichments have been reported[39,40]. Finally, the improvements in prediction accuracy that we reported are a function of the baseline-LD model[17], but there are many possible ways to improve this model, e.g. by incorporating tissue-specific enrichments[1–6,41–44], modeling MAF-dependent architectures[45,46], and/or employing alternative approaches to modeling LD-dependent effects[34]; we anticipate that future improvements to the baseline-LD model will yield even larger improvements in prediction accuracy. As an initial step to explore alternative approaches to modeling LD-dependent effects, we repeated our analyses using the baseline-LD+LDAK model (introduced in ref. 33), which consists of the baseline-LD model plus one additional continuous annotation constructed using LDAK weights[34]. (Recent work has shown that incorporating LDAK weights increases polygenic prediction accuracy in analyses that do not include the baseline-LD model[47].) We determined that results were virtu-

ally unchanged (avg prediction R^2=0.1600 for baseline-LD+LDAK vs. 0.1601 for baseline-LD using LDpred-funct-inf with UK10K SNPs; see Table S8 and Table S12). Despite these limitations and open directions for future research, our work unequivocally demonstrates that leveraging functional enrichment using the baseline-LD model substantially improves polygenic prediction accuracy.

Acknowledgements

We thank the research participants and employees of 23andMe for making this work possible. We are grateful to S. Sunyaev, S. Chun, L. O'Connor, O. Weissbrod and H. Finucane for helpful discussions. This research was conducted using the UK Biobank Resource under Application #16549 and was funded by NIH grants R01 GM105857, R01 MH101244 and U01 HG009379.

Collaborators for the 23andMe research team are: Michelle Agee, Babak Alipanahi, Robert K. Bell, Katarzyna Bryc, Sarah L. Elson, Pierre Fontanillas, David A. Hinds, Jennifer C. McCreight, Karen E. Huber, Aaron Kleinman, Nadia K. Litterman, Matthew H. McIntyre, Joanna L. Mountain, Elizabeth S. Noblin, Carrie A.M. Northover, Steven J. Pitts, J. Fah Sathirapongsasuti, Olga V. Sazonova, Janie F. Shelton, Suyash Shringarpure, Chao Tian, Joyce Y. Tung, Vladimir Vacic, and Catherine H. Wilson.

Web Resources

Software implementing the LDpred-funct-inf and LDpred-funct methods will be released prior to publication as a publicly available, open-source software package: `https://www.hsph.harvard.edu/alkes-price/software`

LDscore regression software: `https://github.com/bulik/ldsc`

UK Biobank Resource: `http://www.ukbiobank.ac.uk/`

BOLT-LMM v2.3 software `http://data.broadinstitute.org/alkesgroup/BOLT-LMM/`

BOLT-LMM v2.3 association statistics: `https://data.broadinstitute.org/alkesgroup/UKBB/UKBB_409K/`

23andMe height association statistics: The full summary statistics for the 23andMe height GWAS will be made available through 23andMe to qualified researchers under an agreement with 23andMe that protects the privacy of the 23andMe participants. Please visit `https://research.23andme.com/collaborate/#publication` for more information and to apply to access the data.

References

[1] Matthew T Maurano, Richard Humbert, Eric Rynes, Robert E Thurman, Eric Haugen, Hao Wang, Alex P Reynolds, Richard Sandstrom, Hongzhu Qu, Jennifer Brody, et al. Systematic localization of common disease-associated variation in regulatory dna. *Science*, page 1222794, 2012.

[2] Gosia Trynka, Cynthia Sandor, Buhm Han, Han Xu, Barbara E Stranger, X Shirley Liu, and Soumya Raychaudhuri. Chromatin marks identify critical cell types for fine mapping complex trait variants. *Nature genetics*, 45(2):124, 2013.

[3] Joseph K Pickrell. Joint analysis of functional genomic data and genome-wide association studies of 18 human traits. *American Journal of Human Genetics*, 94(4):559–573, 04 2014.

[4] Roadmap Epigenomics Consortium, Anshul Kundaje, Wouter Meuleman, Jason Ernst, Misha Bilenky, Angela Yen, Alireza Heravi-Moussavi, Pouya Kheradpour, Zhizhuo Zhang, Jianrong Wang, Michael J. Ziller, Viren Amin, John W. Whitaker, Matthew D. Schultz, Lucas D. Ward, Abhishek Sarkar, Gerald Quon, Richard S. Sandstrom, Matthew L. Eaton, Yi-Chieh Wu, Andreas R. Pfenning, Xinchen Wang, Melina Claussnitzer, Yaping Liu, Cristian Coarfa, R. Alan Harris, Noam Shoresh, Charles B. Epstein, Elizabeta Gjoneska, Danny Leung, Wei Xie, R. David Hawkins, Ryan Lister, Chibo Hong, Philippe Gascard, Andrew J. Mungall, Richard Moore, Eric Chuah, Angela Tam, Theresa K. Canfield, R. Scott Hansen, Rajinder Kaul, Peter J. Sabo, Mukul S. Bansal, Annaick Carles, Jesse R. Dixon, Kai-How Farh, Soheil Feizi, Rosa Karlic, Ah-Ram Kim, Ashwinikumar Kulkarni, Daofeng Li, Rebecca Lowdon, GiNell Elliott, Tim R. Mercer, Shane J. Neph, Vitor Onuchic, Paz Polak, Nisha Rajagopal, Pradipta Ray, Richard C. Sallari, Kyle T. Siebenthall, Nicholas A. Sinnott-Armstrong, Michael Stevens, Robert E. Thurman, Jie Wu, Bo Zhang, Xin Zhou, Arthur E. Beaudet, Laurie A. Boyer, Philip L. De Jager, Peggy J. Farnham, Susan J. Fisher, David Haussler, Steven J. M. Jones, Wei Li, Marco A. Marra, Michael T. McManus, Shamil Sunyaev, James A. Thomson, Thea D. Tlsty, Li-Huei Tsai, Wei Wang, Robert A. Waterland, Michael Q. Zhang, Lisa H. Chadwick, Bradley E. Bernstein, Joseph F. Costello, Joseph R. Ecker, Martin Hirst, Alexander Meissner, Aleksandar Milosavljevic, Bing Ren, John A. Stamatoyannopoulos, Ting Wang, and Manolis Kellis. Integrative analysis of 111 reference human epigenomes. *Nature*, 518:317 EP –, 02 2015.

[5] Hilary K Finucane, Brendan Bulik-Sullivan, Alexander Gusev, Gosia Trynka, Yakir Reshef, Po-Ru Loh, Verneri Anttila, Han Xu, Chongzhi Zang, Kyle Farh, Stephan Ripke, Felix R Day, ReproGen Consortium, Schizophrenia Working Group of the Psychiatric Genomics Consortium, The RACI Consortium, Shaun Purcell, Eli Stahl, Sara Lindstrom, John R B Perry, Yukinori

Okada, Soumya Raychaudhuri, Mark J Daly, Nick Patterson, Benjamin M Neale, and Alkes L Price. Partitioning heritability by functional annotation using genome-wide association summary statistics. *Nature Genetics*, 47:1228 EP –, 09 2015.

[6] Kyle Kai-How Farh, Alexander Marson, Jiang Zhu, Markus Kleinewietfeld, William J Housley, Samantha Beik, Noam Shoresh, Holly Whitton, Russell JH Ryan, Alexander A Shishkin, et al. Genetic and epigenetic fine mapping of causal autoimmune disease variants. *Nature*, 518(7539):337, 2015.

[7] Nilanjan Chatterjee, Jianxin Shi, and Montserrat García-Closas. Developing and evaluating polygenic risk prediction models for stratified disease prevention. *Nature Reviews Genetics*, 17:392 EP –, 05 2016.

[8] Xiang Zhou, Peter Carbonetto, and Matthew Stephens. Polygenic modeling with bayesian sparse linear mixed models. *PLOS Genetics*, 9(2):1–14, 02 2013.

[9] Gerhard Moser, Sang Hong Lee, Ben J. Hayes, Michael E. Goddard, Naomi R. Wray, and Peter M. Visscher. Simultaneous discovery, estimation and prediction analysis of complex traits using a bayesian mixture model. *PLOS Genetics*, 11(4):1–22, 04 2015.

[10] Doug Speed and David J Balding. Multiblup: improved snp-based prediction for complex traits. *Genome Research*, 24(9):1550–1557, 09 2014.

[11] Bjarni J Vilhjálmsson, Jian Yang, Hilary K Finucane, Alexander Gusev, Sara Lindström, Stephan Ripke, Giulio Genovese, Po-Ru Loh, Gaurav Bhatia, Ron Do, et al. Modeling linkage disequilibrium increases accuracy of polygenic risk scores. *The American Journal of Human Genetics*, 97(4):576–592, 2015.

[12] C. R. Henderson. Best linear unbiased estimation and prediction under a selection model. *Biometrics*, 31(2):423–447, 1975.

[13] International Schizophrenia Consortium, Shaun M. Purcell, Naomi R. Wray, Jennifer L. Stone, Peter M. Visscher, Michael C. O'Donovan, Patrick F. Sullivan, and Pamela Sklar. Common polygenic variation contributes to risk of schizophrenia and bipolar disorder. *Nature*, 460(7256):748–752, August 2009.

[14] Eli A Stahl, Daniel Wegmann, Gosia Trynka, Javier Gutierrez-Achury, Ron Do, Benjamin F Voight, Peter Kraft, Robert Chen, Henrik J Kallberg, Fina AS Kurreeman, et al. Bayesian inference analyses of the polygenic architecture of rheumatoid arthritis. *Nature genetics*, 44(5):483–489, 2012.

[15] Jianxin Shi, Ju-Hyun Park, Jubao Duan, Berndt, et al. Winner's Curse Correction and Variable Thresholding Improve Performance of Polygenic Risk Modeling Based on Genome-Wide Association Study Summary-Level Data. *PLOS Genetics*, 12(12):e1006493, December 2016.

[16] Yiming Hu, Qiongshi Lu, Ryan Powles, Xinwei Yao, Can Yang, Fang Fang, Xinran Xu, and Hongyu Zhao. Leveraging functional annotations in genetic risk prediction for human complex diseases. *PLOS Computational Biology*, 13(6):1–16, 06 2017.

[17] Steven Gazal, Hilary K Finucane, Nicholas A Furlotte, Po-Ru Loh, Pier Francesco Palamara, Xuanyao Liu, Armin Schoech, Brendan Bulik-Sullivan, Benjamin M Neale, Alexander Gusev, and Alkes L Price. Linkage disequilibrium–dependent architecture of human complex traits shows action of negative selection. *Nature Genetics*, 49:1421 EP –, 09 2017.

[18] Nilanjan Chatterjee, Jianxin Shi, and Montserrat GarcÃa-Closas. Developing and evaluating polygenic risk prediction models for stratified disease prevention. *Nat Rev Genet*, 17(7):392–406, July 2016.

[19] Carla Marquez-Luna, The SIGMA Type 2 Diabetes Consortium, and Alkes L. Price. Multi-ethnic polygenic risk scores improve risk prediction in diverse populations. *bioRxiv*, page 051458, May 2016.

[20] Po-Ru Loh, Gleb Kichaev, Steven Gazal, Armin P Schoech, and Alkes L Price. Mixed-model association for biobank-scale datasets. *Nature Genetics*, page Epub June 11, 2018.

[21] Tian Ge, Chia-Yen Chen, Benjamin M. Neale, Mert R. Sabuncu, and Jordan W. Smoller. Phenome-wide heritability analysis of the UK Biobank. *PLOS Genetics*, 13(4):e1006711, April 2017.

[22] Gilbert Strang. *Linear Algebra and Its Applications*. Academic Press, Inc., 2nd edition, 1980.

[23] Sung Chun, Maxim Imakaev, Nathan O Stitziel, and Shamil R Sunyaev. Non-parametric polygenic risk prediction using partitioned gwas summary statistics. *bioRxiv*, 01 2018.

[24] Naomi R. Wray, Jian Yang, Ben J. Hayes, Alkes L. Price, Michael E. Goddard, and Peter M. Visscher. Pitfalls of predicting complex traits from snps. *Nature Reviews Genetics*, 14:507 EP –, 06 2013.

[25] Clare Bycroft, Colin Freeman, Desislava Petkova, Gavin Band, Lloyd T Elliott, Kevin Sharp, Allan Motyer, Damjan Vukcevic, Olivier Delaneau, Jared O'Connell, Adrian Cortes, Samantha Welsh, Gil McVean, Stephen Leslie, Peter Donnelly, and Jonathan Marchini. Genome-wide genetic data on 500,000 uk biobank participants. *bioRxiv*, 2017.

[26] Cathie Sudlow, John Gallacher, Naomi Allen, Valerie Beral, Paul Burton, John Danesh, Paul Downey, Paul Elliott, Jane Green, Martin Landray, et al. Uk biobank: an open access resource for identifying the causes of a wide range of complex diseases of middle and old age. *PLoS medicine*, 12(3):e1001779, 2015.

[27] Kevin J. Galinsky, Po-Ru Loh, Swapan Mallick, Nick J. Patterson, and Alkes L. Price. Population structure of uk biobank and ancient eurasians reveals adaptation at genes influencing blood pressure. *The American Journal of Human Genetics*, 99(5):1130–1139, 11 2016.

[28] Kevin J. Galinsky, Gaurav Bhatia, Po-Ru Loh, Stoyan Georgiev, Sayan Mukherjee, Nick J. Patterson, and Alkes L. Price. Fast Principal-Component Analysis Reveals Convergent Evolution of ADH1b in Europe and East Asia. *The American Journal of Human Genetics*, 98(3):456–472, March 2016.

[29] Eric Y Durand, Chuong B Do, Joanna L Mountain, and J. Michael Macpherson. Ancestry composition: A novel, efficient pipeline for ancestry deconvolution. *bioRxiv*, 2014.

[30] Carla Márquez-Luna, Po-Ru Loh, South Asian Type 2 Diabetes (SAT2D) Consortium, The SIGMA Type 2 Diabetes Consortium, and Alkes L. Price. Multiethnic polygenic risk scores improve risk prediction in diverse populations. *Genetic Epidemiology*, 41(8):811–823, 2017.

[31] 1000 Genomes Project Consortium et al. A global reference for human genetic variation. *Nature*, 526(7571):68, 2015.

[32] UK10K Consortium et al. The uk10k project identifies rare variants in health and disease. *Nature*, 526(7571):82, 2015.

[33] Steven Gazal, Hilary K Finucane, and Alkes L Price. Reconciling s-ldsc and ldak functional enrichment estimates. *bioRxiv*, 2018.

[34] Doug Speed, Na Cai, Michael R Johnson, Sergey Nejentsev, David J Balding, UCLEB Consortium, et al. Reevaluation of snp heritability in complex human traits. *Nature genetics*, 49(7):986, 2017.

[35] Bogdan Pasaniuc and Alkes L Price. Dissecting the genetics of complex traits using summary association statistics. *Nature Reviews Genetics*, 18(2):117, 2017.

[36] Robert Maier, Gerhard Moser, Guo-Bo Chen, Stephan Ripke, Cross-Disorder Working Group of the Psychiatric Genomics Consortium, William Coryell, James B. Potash, William A. Scheftner, Jianxin Shi, Myrna M. Weissman, Christina M. Hultman, Mikael LandÃ©n, Douglas F. Levinson, Kenneth S. Kendler, Jordan W. Smoller, Naomi R. Wray, and S. Hong Lee. Joint analysis

of psychiatric disorders increases accuracy of risk prediction for schizophrenia, bipolar disorder, and major depressive disorder. *Am. J. Hum. Genet.*, 96(2):283–294, February 2015.

[37] Robert M. Maier, Zhihong Zhu, Sang Hong Lee, Maciej Trzaskowski, Douglas M. Ruderfer, Eli A. Stahl, Stephan Ripke, Naomi R. Wray, Jian Yang, Peter M. Visscher, and Matthew R. Robinson. Improving genetic prediction by leveraging genetic correlations among human diseases and traits. *Nature Communications*, 9(1):989, 2018.

[38] George Tucker, Po-Ru Loh, Iona M. MacLeod, Ben J. Hayes, Michael E. Goddard, Bonnie Berger, and Alkes L. Price. Two-Variance-Component Model Improves Genetic Prediction in Family Datasets. *Am. J. Hum. Genet.*, 97(5):677–690, November 2015.

[39] Gleb Kichaev, Gaurav Bhatia, Po-Ru Loh Loh, Steven Gazal, Kathryn Burch, Malika Freund, Armin Schoech, Bogdan Pasaniuc, and Alkes L. Price. Leveraging polygenic functional enrichment to improve gwas power. *Submitted*.

[40] Masahiro Kanai, Masato Akiyama, Atsushi Takahashi, Nana Matoba, Yukihide Momozawa, Masashi Ikeda, Nakao Iwata, Shiro Ikegawa, Makoto Hirata, Koichi Matsuda, Michiaki Kubo, Yukinori Okada, and Yoichiro Kamatani. Genetic analysis of quantitative traits in the Japanese population links cell types to complex human diseases. *Nature Genetics*, 50(3):390–400, March 2018.

[41] Diego Calderon, Anand Bhaskar, David A. Knowles, David Golan, Towfique Raj, Audrey Q. Fu, and Jonathan K. Pritchard. Inferring Relevant Cell Types for Complex Traits by Using Single-Cell Gene Expression. *Am. J. Hum. Genet.*, 101(5):686–699, November 2017.

[42] Halit Ongen, Andrew A. Brown, Olivier Delaneau, Nikolaos I. Panousis, Alexandra C. Nica, GTEx Consortium, and Emmanouil T. Dermitzakis. Estimating the causal tissues for complex traits and diseases. *Nat. Genet.*, 49(12):1676–1683, December 2017.

[43] Hilary K. Finucane, Yakir A. Reshef, Verneri Anttila, Kamil Slowikowski, Alexander Gusev, Andrea Byrnes, Steven Gazal, Po-Ru Loh, Caleb Lareau, Noam Shoresh, Giulio Genovese, Arpiar Saunders, Evan Macosko, Samuela Pollack, Brainstorm Consortium, John R. B. Perry, Jason D. Buenrostro, Bradley E. Bernstein, Soumya Raychaudhuri, Steven McCarroll, Benjamin M. Neale, and Alkes L. Price. Heritability enrichment of specifically expressed genes identifies disease-relevant tissues and cell types. *Nat. Genet.*, 50(4):621–629, April 2018.

[44] Daniel Backenroth, Zihuai He, Krzysztof Kiryluk, Valentina Boeva, Lynn Pethukova, Ekta Khurana, Angela Christiano, Joseph D. Buxbaum, and Iuliana Ionita-Laza. FUN-LDA: A Latent Dirichlet Allocation Model for Predicting Tissue-Specific Functional Effects of Noncoding Variation: Methods and Applications. *Am. J. Hum. Genet.*, 102(5):920–942, May 2018.

[45] Armin Schoech, Daniel Jordan, Po-Ru Loh, Steven Gazal, Luke O'Connor, Daniel J. Balick, Pier F. Palamara, Hilary Finucane, Shamil R. Sunyaev, and Alkes L. Price. Quantification of frequency-dependent genetic architectures and action of negative selection in 25 UK Biobank traits. *bioRxiv*, page 188086, September 2017.

[46] Jian Zeng, Ronald de Vlaming, Yang Wu, Matthew R. Robinson, Luke R. Lloyd-Jones, Loic Yengo, Chloe X. Yap, Angli Xue, Julia Sidorenko, Allan F. McRae, Joseph E. Powell, Grant W. Montgomery, Andres Metspalu, Tonu Esko, Greg Gibson, Naomi R. Wray, Peter M. Visscher, and Jian Yang. Signatures of negative selection in the genetic architecture of human complex traits. *Nature Genetics*, 50(5):746–753, May 2018.

[47] Doug Speed and David Balding. Better estimation of snp heritability from summary statistics provides a new understanding of the genetic architecture of complex traits. *bioRxiv*, 2018.

Figures

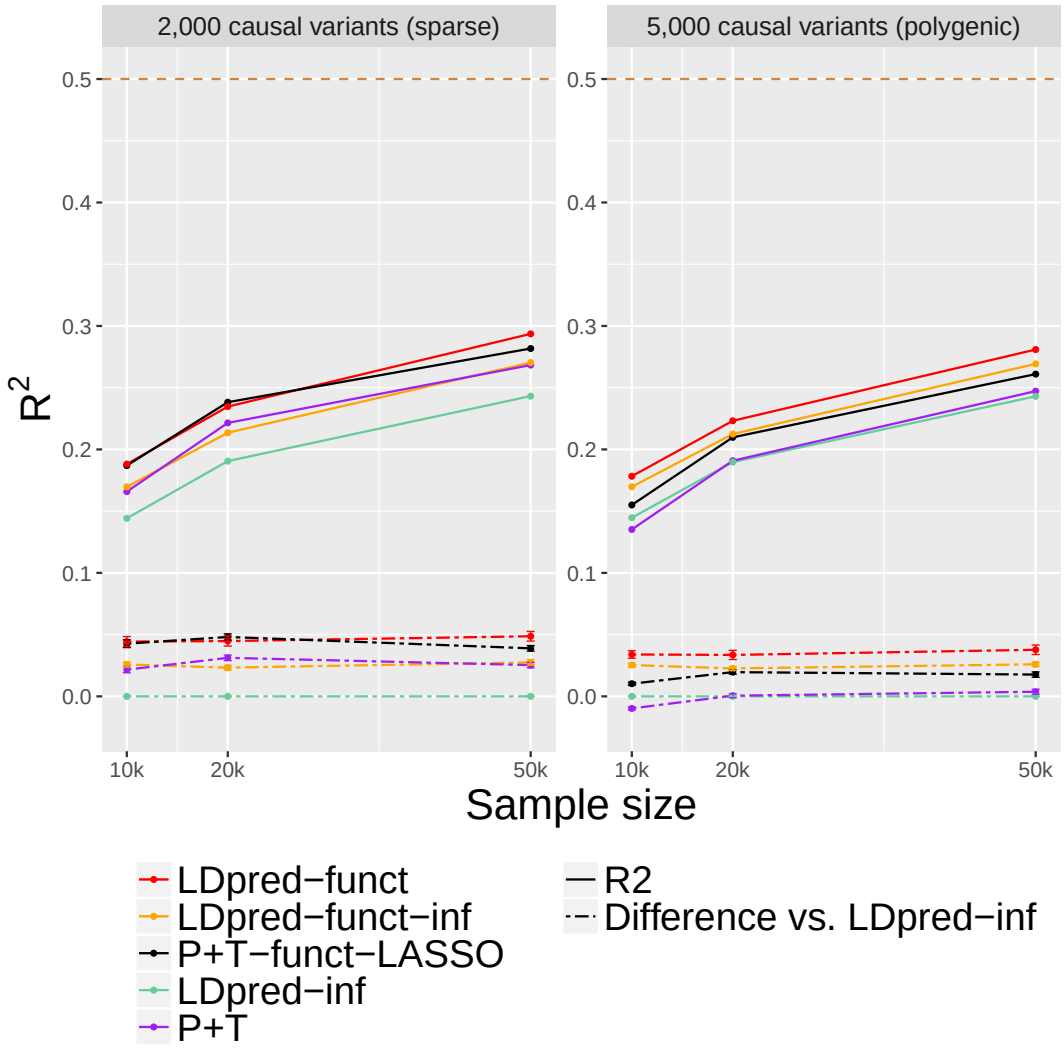

Figure 1: Accuracy of 5 polygenic prediction methods in simulations using UK Biobank genotypes. We report results for P+T, LDpred-inf, P+T-funct-LASSO, LDpred-funct-inf and LDpred-funct in chromosome 1 simulations with 2,000 causal variants (sparse architecture) and 5,000 causal variants (polygenic architecture). Results are averaged across 100 simulations. Top dashed line denotes simulated SNP-heritability of 0.5. Bottom dashed lines denote differences vs. LDpred-inf; error bars represent 95% confidence intervals. Results for other values of the number of causal variants are reported in Figure S1, and numerical results are reported in Table S2 and Table S3.

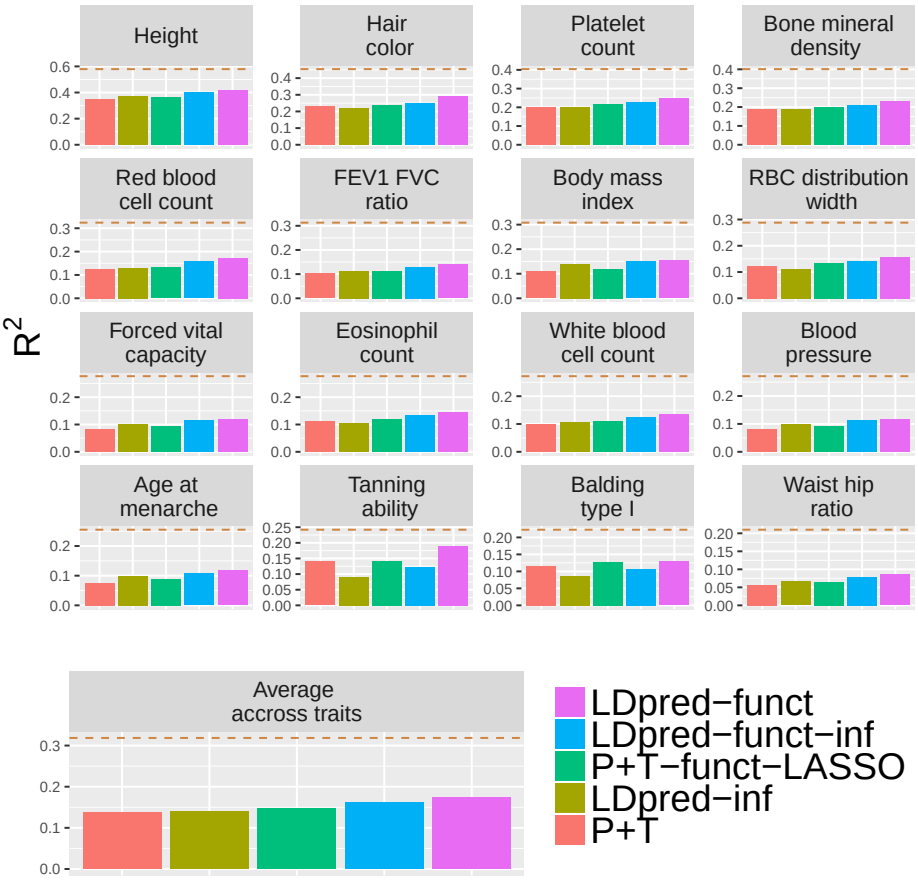

Figure 2: Accuracy of 5 polygenic prediction methods across 16 UK Biobank traits. We report results for P+T, LDpred-inf, P+T-funct-LASSO, LDpred-funct-inf and LDpred-funct. Dashed lines denote estimates of SNP-heritability. Numerical results are reported in Table S6 and Table S8. Jackknife s.e. for differences vs. LDpred-inf are reported in Table S7; for Average across traits, each jackknife s.e. is < 0.0009.

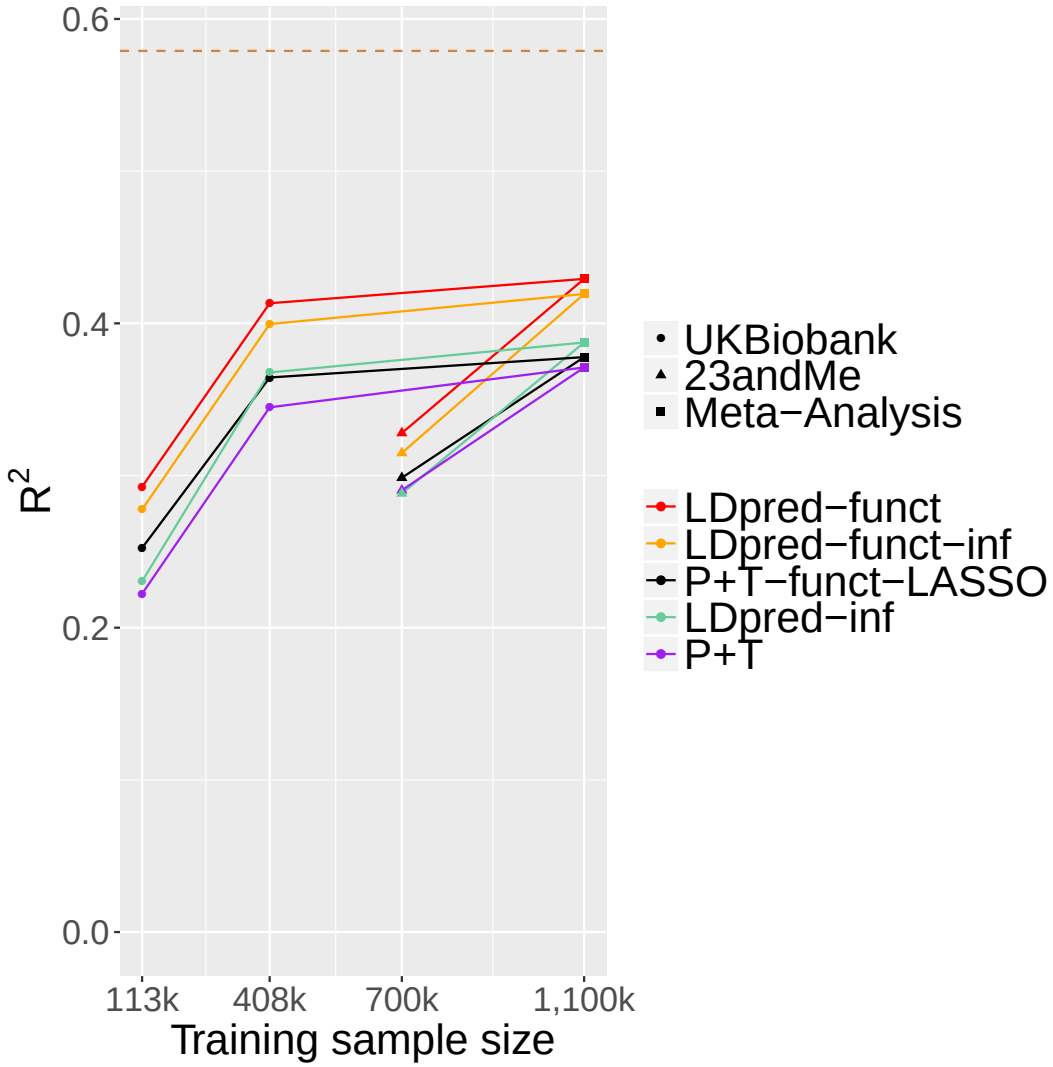

Figure 3: Accuracy of 5 prediction methods in height meta-analysis of UK Biobank and 23andMe cohorts. We report results for P+T, LDpred-inf, P+T-funct-LASSO, LDpred-funct-inf and LDpred-funct, for each of 4 training data sets: UK Biobank interim release (113,660 training samples), UK Biobank (408,092 training samples), 23andMe (698,430 training samples) and meta-analysis of UK Biobank and 23andMe (1,107,430 training samples). Nested training data sets are connected by solid lines. Dashed line denotes estimate of SNP-heritability in UK Biobank. Numerical results are reported in Table S11.

Supplementary Figures

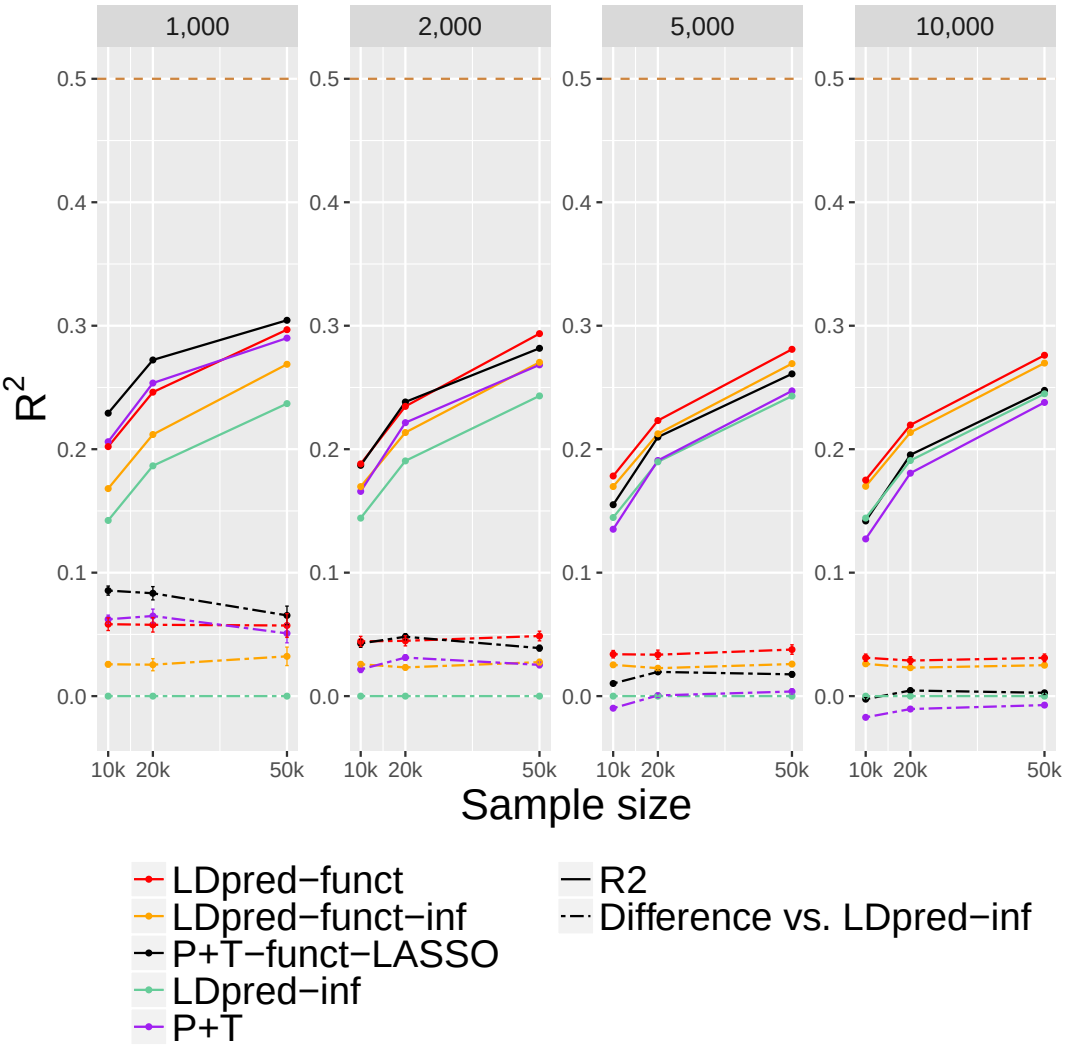

Figure S1: Accuracy of 5 polygenic prediction methods in simulations using UK Biobank genotypes, for 4 values of the number of causal variants. We report results for P+T, LDpred-inf, P+T-funct-LASSO, LDpred-funct-inf and LDpred-funct in chromosome 1 simulations with 1,000 causal variants (extremely sparse architecture), 2,000 causal variants (sparse architecture), 5,000 causal variants (polygenic architecture) and 10,000 causal variants (extremely polygenic architecture). Results are averaged across 100 simulations. Top dashed line denotes simulated SNP-heritability of 0.5. Bottom dashed lines denote differences vs. LDpred-inf; error bars represent 95% confidence intervals. Numerical results are reported in Table S2 and Table S3.

Supplementary Tables

	Trait	Training N	Validation N (ancestry distribution)	
1	Height	408092	25030	(43.5% Irish, 56.5% Other)
2	Hair color	403024	24773	(43.5% Irish, 56.5% Other)
3	Platelet count	395747	24277	(43.5% Irish, 56.5% Other)
4	Bone mineral density	397274	24167	(43.6% Irish, 56.4% Other)
5	Red blood cell count	396464	24305	(43.5% Irish, 56.5% Other)
6	FEV1-FVC ratio	331786	19929	(42.5% Irish, 57.5% Other)
7	Body mass index	407667	25000	(43.5% Irish, 56.5% Other)
8	RBC distribution width	394258	24175	(43.5% Irish, 56.5% Other)
9	Eosinophil count	391787	24030	(43.4% Irish, 56.6% Other)
10	Forced vital capacity	331786	19929	(42.5% Irish, 57.5% Other)
11	White blood cell count	395835	24293	(43.5% Irish, 56.5% Other)
12	Blood pressure	376437	23127	(43.2% Irish, 56.8% Other)
13	Age at menarche	214860	13999	(39.7% Irish, 60.3% Other)
14	Tanning ability	400721	24608	(43.5% Irish, 56.5% Other)
15	Balding type I	186506	10578	(48.9% Irish, 51.1% Other)
16	Waist hip ratio	408196	25032	(43.5% Irish, 56.5% Other)

Table S1: List of 16 UK Biobank traits. We list the training sample size and validation sample size for each trait.

# Causal variants	Model	Training sample size 10,000 Average $R^2(s.e.)$	20,000 Average $R^2(s.e.)$	50,000 Average $R^2(s.e.)$
1,000	P+T	0.2061 (0.0022)	0.2536 (0.0021)	0.2900 (0.0019)
	LDpred-inf	0.1423 (0.0020)	0.1865 (0.0031)	0.2369 (0.0045)
	P+T-funct-LASSO	0.2292 (0.0024)	0.2723 (0.0024)	0.3044 (0.002)
	LDpred-funct-inf	0.1681 (0.0024)	0.2119 (0.0028)	0.2688 (0.0033)
	LDpred-funct	0.2021 (0.0021)	0.2462 (0.0019)	0.2968 (0.0025)
2,000	P+T	0.1658 (0.0022)	0.2215 (0.0026)	0.2683 (0.0029)
	LDpred-inf	0.1442 (0.0019)	0.1905 (0.0023)	0.2432 (0.0028)
	P+T-funct-LASSO	0.1869 (0.0026)	0.2383 (0.0028)	0.2817 (0.0031)
	LDpred-funct-inf	0.1697 (0.0022)	0.2135 (0.0026)	0.2703 (0.003)
	LDpred-funct	0.1881 (0.0017)	0.2347 (0.0019)	0.2936 (0.0016)
5,000	P+T	0.1352 (0.0016)	0.1909 (0.0020)	0.2472 (0.0024)
	LDpred-inf	0.1447 (0.0017)	0.1898 (0.0022)	0.2430 (0.0027)
	P+T-funct-LASSO	0.1550 (0.0018)	0.2098 (0.0021)	0.2610 (0.0026)
	LDpred-funct-inf	0.1698 (0.0019)	0.2125 (0.0022)	0.2693 (0.0027)
	LDpred-funct	0.1783 (0.0012)	0.2232 (0.0013)	0.2809 (0.0015)
10,000	P+T	0.1273 (0.0015)	0.1806 (0.002)	0.2379 (0.0024)
	LDpred-inf	0.1442 (0.0017)	0.1908 (0.0021)	0.2449 (0.0026)
	P+T-funct-LASSO	0.1419 (0.0017)	0.1954 (0.0022)	0.2477 (0.0026)
	LDpred-funct-inf	0.1700 (0.0020)	0.2136 (0.0023)	0.2698 (0.0028)
	LDpred-funct	0.1750 (0.0012)	0.2196 (0.0012)	0.2761 (0.0013)

Table S2: Accuracy of 5 polygenic prediction methods in simulations using UK Biobank genotypes, for 4 values of the number of causal variants. We report results for P+T, LDpred-inf, P+T-funct-LASSO, LDpred-funct-inf and LDpred-funct in chromosome 1 simulations with 1,000 causal variants (extremely sparse architecture), 2,000 causal variants (sparse architecture), 5,000 causal variants (polygenic architecture) and 10,000 causal variants (extremely polygenic architecture). Results are averaged across 100 simulations.

(a)

# Causal variants	Model	Training sample size 10,000 Diff. R^2 (s.e.)	20,000 Diff. R^2 (s.e.)	50,000 Diff. R^2 (s.e.)
1,000	P+T	0.0622 (0.0017)	0.0649 (0.0028)	0.0508 (0.0038)
	LDpred-inf	0.0000 (0.0000)	0.0000 (0.0000)	0.0000 (0.0000)
	P+T-funct-LASSO	0.0855 (0.0018)	0.0833 (0.0027)	0.0654 (0.0038)
	LDpred-funct-inf	0.0258 (0.0010)	0.0255 (0.0025)	0.0322 (0.0038)
	LDpred-funct	0.0583 (0.0026)	0.0578 (0.0030)	0.0572 (0.0048)
2,000	P+T	0.0216 (0.0012)	0.0312 (0.0011)	0.0253 (0.0011)
	LDpred-inf	0.0000 (0.0000)	0.0000 (0.0000)	0.0000 (0.0000)
	P+T-funct-LASSO	0.0427 (0.0016)	0.0481 (0.0012)	0.0389 (0.0011)
	LDpred-funct-inf	0.0258 (0.0010)	0.0233 (0.0010)	0.0275 (0.0011)
	LDpred-funct	0.0443 (0.0021)	0.0448 (0.0021)	0.0487 (0.0020)
5,000	P+T	-0.0098 (0.0006)	0.0006 (0.0008)	0.0037 (0.0010)
	LDpred-inf	0.0000 (0.0000)	0.0000 (0.0000)	0.0000 (0.0000)
	P+T-funct-LASSO	0.0103 (0.0007)	0.0196 (0.0008)	0.0177 (0.0011)
	LDpred-funct-inf	0.0254 (0.0008)	0.0226 (0.0008)	0.026 (0.0009)
	LDpred-funct	0.0339 (0.0015)	0.0336 (0.0019)	0.0377 (0.0019)
10,000	P+T	-0.0172 (0.0007)	-0.0104 (0.0007)	-0.0072 (0.0008)
	LDpred-inf	0.0000 (0.0000)	0.0000 (0.0000)	0.0000 (0.0000)
	P+T-funct-LASSO	-0.0024 (0.0007)	0.0046 (0.0008)	0.0027 (0.0009)
	LDpred-funct-inf	0.0262 (0.0008)	0.0230 (0.0008)	0.0250 (0.0007)
	LDpred-funct	0.0311 (0.0015)	0.0288 (0.0016)	0.031 (0.0016)

(b)

# Causal variants	Model	Training sample size 10,000 Diff. R^2 (s.e.)	20,000 Diff. R^2 (s.e.)	50,000 Diff. R^2 (s.e.)
1,000	P+T	-0.004 (0.0029)	-0.0071 (0.0027)	0.0064 (0.0034)
	LDpred-inf	0.0583 (0.0026)	0.0578 (0.003)	0.0572 (0.0048)
	P+T-funct-LASSO	-0.0272 (0.003)	-0.0255 (0.0028)	-0.0082 (0.0035)
	LDpred-funct-inf	0.0325 (0.0028)	0.0323 (0.0025)	0.025 (0.0034)
	LDpred-funct	0.0000 (0.0000)	0.0000 (0.0000)	0.0000 (0.0000)
2,000	P+T	0.0227 (0.0024)	0.0136 (0.0023)	0.0234 (0.0023)
	LDpred-inf	0.0443 (0.0021)	0.0448 (0.0021)	0.0487 (0.002)
	P+T-funct-LASSO	0.0017 (0.0026)	-0.0033 (0.0023)	0.0098 (0.0023)
	LDpred-funct-inf	0.0185 (0.0021)	0.0215 (0.002)	0.0212 (0.0022)
	LDpred-funct	0.0000 (0.0000)	0.0000 (0.0000)	0.0000 (0.0000)
5,000	P+T	0.0437 (0.0016)	0.033 (0.0018)	0.034 (0.0018)
	LDpred-inf	0.0339 (0.0015)	0.0336 (0.0019)	0.0377 (0.0019)
	P+T-funct-LASSO	0.0237 (0.0016)	0.0139 (0.0018)	0.0201 (0.0019)
	LDpred-funct-inf	0.0086 (0.0015)	0.0109 (0.0017)	0.0118 (0.0018)
	LDpred-funct	0.0000 (0.0000)	0.0000 (0.0000)	0.0000 (0.0000)
10,000	P+T	0.0483 (0.0014)	0.0393 (0.0015)	0.0382 (0.0016)
	LDpred-inf	0.0311 (0.0015)	0.0288 (0.0016)	0.031 (0.0016)
	P+T-funct-LASSO	0.0336 (0.0015)	0.0243 (0.0016)	0.0283 (0.0017)
	LDpred-funct-inf	0.0049 (0.0015)	0.0058 (0.0016)	0.006 (0.0017)
	LDpred-funct	0.0000 (0.0000)	0.0000 (0.0000)	0.0000 (0.0000)

Table S3: Differences between polygenic prediction methods in simulations using UK Biobank genotypes, for 4 values of the number of causal variants. We report results for P+T, LDpred-inf, P+T-funct-LASSO, LDpred-funct-inf and LDpred-funct in chromosome 1 simulations with 1,000 causal variants (extremely sparse architecture), 2,000 causal variants (sparse architecture), 5,000 causal variants (polygenic architecture) and 10,000 causal variants (extremely polygenic architecture). Results are averaged across 100 simulations. (a) Difference between R^2 for each method vs. R^2 for LDpred-inf. (b) Difference between R^2 for LDpred-funct vs. R^2 for each method.

# Causal variants	Model	Training sample size 10,000 Average $R^2(s.e.)$	20,000 Average $R^2(s.e.)$	50,000 Average $R^2(s.e.)$
1,000	LDpred-funct-inf	0.1681 (0.0024)	0.2119 (0.0028)	0.2688 (0.0033)
	LDpred-funct-10	0.1958 (0.002)	0.2402 (0.0019)	0.2937 (0.0019)
	LDpred-funct-20	0.2021 (0.0021)	0.2462 (0.0019)	0.2968 (0.0025)
	LDpred-funct-50	0.2130 (0.0021)	0.2561 (0.0021)	0.3089 (0.0021)
	LDpred-funct-100	0.2243 (0.0022)	0.2647 (0.0025)	0.2976 (0.0074)
2,000	LDpred-funct-inf	0.1697 (0.0022)	0.2135 (0.0026)	0.2703 (0.0030)
	LDpred-funct-10	0.1840 (0.0024)	0.2296 (0.0027)	0.2912 (0.0015)
	LDpred-funct-20	0.1881 (0.0024)	0.2347 (0.0028)	0.2936 (0.0015)
	LDpred-funct-50	0.1978 (0.0025)	0.2439 (0.0028)	0.3005 (0.0017)
	LDpred-funct-100	0.2054 (0.0028)	0.2528 (0.0028)	0.3019 (0.0054)
5,000	LDpred-funct-inf	0.1698 (0.0019)	0.2125 (0.0022)	0.2693 (0.0027)
	LDpred-funct-10	0.1758 (0.0019)	0.2206 (0.0023)	0.2788 (0.0028)
	LDpred-funct-20	0.1783 (0.0019)	0.2232 (0.0023)	0.2809 (0.0028)
	LDpred-funct-50	0.1836 (0.0019)	0.229 (0.0024)	0.2861 (0.0028)
	LDpred-funct-100	0.1899 (0.002)	0.2344 (0.0026)	0.2915 (0.0028)
10,000	LDpred-funct-inf	0.1700 (0.0020)	0.2136 (0.0023)	0.2698 (0.0028)
	LDpred-funct-10	0.1746 (0.0012)	0.2199 (0.0012)	0.2746 (0.0028)
	LDpred-funct-20	0.1750 (0.002)	0.2196 (0.0023)	0.2761 (0.0028)
	LDpred-funct-50	0.1799 (0.002)	0.2240 (0.0024)	0.2800 (0.0028)
	LDpred-funct-100	0.1849 (0.0021)	0.2289 (0.0024)	0.2835 (0.0029)

Table S4: Sensitivity of LDpred-funct results to number of bins used for regularization in simulations using UK Biobank genotypes. We report results with the number of posterior mean causal effect size bins used for regularization (K) set to 10, 20, 50 or 100. LDpred-funct-K denotes each respective value of K. We also report results for LDpred-funct-inf, which is identical to LDpred-funct with K set to 1. Results are averaged across 100 simulations.

	Trait	Training N	h_g^2	c
1	Height	408092	0.58	0.45
2	Hair color	403024	0.45	0.23
3	Platelet count	395747	0.40	0.30
4	Bone mineral density	397274	0.40	0.27
5	Red blood cell count	396464	0.32	0.22
6	FEV1-FVC ratio	331786	0.31	0.24
7	Body mass index	407667	0.31	0.28
8	RBC distribution width	394258	0.29	0.20
9	Eosinophil count	391787	0.28	0.19
10	Forced vital capacity	331786	0.28	0.22
11	White blood cell count	395835	0.27	0.22
12	Blood pressure	376437	0.27	0.21
13	Age at menarche	214860	0.26	0.20
14	Tanning ability	400721	0.24	0.09
15	Balding type I	186506	0.22	0.11
16	Waist hip ratio	408196	0.21	0.16

Table S5: Parameter values for 16 UK Biobank traits. For each trait, we list the training sample size, h_g^2 estimate (from BOLT-LMM v2.3; used by LDpred-inf, LDpred-funct-inf and LDpred-funct) and c parameter (used by LDpred-funct-inf and LDpred-funct).

	Trait	h2g	P+T	LDpred-inf	P+T-funct-LASSO	LDpred -funct-inf	LDpred -funct
1	Height	0.579	0.3462	0.3717	0.3667	0.4019	0.4167
2	Hair color	0.454	0.2339	0.2191	0.2389	0.2472	0.2883
3	Platelet count	0.404	0.1994	0.1982	0.2150	0.2290	0.2460
4	Bone mineral density	0.401	0.1871	0.1887	0.1993	0.2105	0.2232
5	Red blood cell count	0.324	0.1247	0.1291	0.1326	0.1572	0.1673
6	FEV1-FVC ratio	0.313	0.1029	0.1139	0.1142	0.1306	0.1345
7	Body mass index	0.308	0.1087	0.1407	0.1189	0.1501	0.1481
8	RBC distribution width	0.288	0.1237	0.1118	0.1346	0.1429	0.1525
9	Eosinophil count	0.277	0.1131	0.1026	0.1189	0.1336	0.1394
10	Forced Vital Capacity	0.277	0.0817	0.1002	0.0935	0.1148	0.1136
11	White blood cell count	0.272	0.0994	0.1054	0.1109	0.1249	0.1282
12	Blood pressure	0.271	0.0802	0.0991	0.0919	0.1111	0.1111
13	Age at menarche	0.255	0.0747	0.0989	0.0899	0.1071	0.1120
14	Tanning ability ability	0.242	0.1405	0.0913	0.1430	0.1234	0.1864
15	Balding type I	0.223	0.1158	0.0874	0.1269	0.1065	0.1235
16	Waist hip ratio	0.210	0.0567	0.0664	0.0645	0.0786	0.0789

Table S6: Accuracy of 5 polygenic prediction methods across 16 UK Biobank traits. We report results for P+T, LDpred-inf, P+T-funct-LASSO, LDpred-funct-inf and LDpred-funct. Jackknife s.e. for differences vs. LDpred-inf are reported in Table S7. Results for Average across traits are reported in Table S8.

	Trait	h_g^2	P+T	LDpred-inf	P+T-funct-LASSO	LDpred-funct-inf	LDpred-funct
1	Height	0.58	-0.0256 (0.0033)	0.0000	-0.0108 (0.0030)	0.0302 (0.0018)	0.0448 (0.0025)
2	Hair color	0.45	0.0148 (0.0038)	0.0000	0.0212 (0.0034)	0.0281 (0.0021)	0.0816 (0.0034)
3	Platelet count	0.40	0.0013 (0.0033)	0.0000	0.0168 (0.0032)	0.0308 (0.0019)	0.0472 (0.0027)
4	Bone mineral density	0.40	-0.0016 (0.0035)	0.0000	0.0106 (0.0030)	0.0217 (0.0016)	0.0342 (0.0024)
5	Red blood cell count	0.32	-0.0044 (0.0033)	0.0000	0.0034 (0.0027)	0.0281 (0.0016)	0.0381 (0.0024)
6	FEV1-FVC ratio	0.31	-0.0110 (0.0035)	0.0000	0.0004 (0.0028)	0.0167 (0.0016)	0.0182 (0.0022)
7	Body mass index	0.31	-0.0320 (0.0025)	0.0000	-0.0242 (0.0024)	0.0094 (0.0014)	0.0077 (0.0016)
8	RBC distribution width	0.29	0.0120 (0.0031)	0.0000	0.0182 (0.0027)	0.0311 (0.0018)	0.0402 (0.0026)
9	Eosinophil count	0.28	0.0105 (0.0031)	0.0000	0.0163 (0.0026)	0.0310 (0.0018)	0.0368 (0.0025)
10	Forced vital capacity	0.28	-0.0185 (0.0029)	0.0000	-0.0067 (0.0025)	0.0146 (0.0015)	0.0101 (0.0018)
11	White blood cell count	0.27	-0.0060 (0.0026)	0.0000	0.0055 (0.0025)	0.0195 (0.0016)	0.0223 (0.0021)
12	Blood pressure	0.27	-0.0189 (0.0026)	0.0000	-0.0071 (0.0024)	0.0120 (0.0014)	0.0117 (0.0018)
13	Age at menarche	0.26	-0.0242 (0.0036)	0.0000	-0.0091 (0.0033)	0.0082 (0.0016)	0.0123 (0.0025)
14	Tanning ability	0.24	0.0492 (0.0033)	0.0000	0.0519 (0.0030)	0.0321 (0.0016)	0.0946 (0.0036)
15	Balding type I	0.22	0.0284 (0.0055)	0.0000	0.0312 (0.0041)	0.0190 (0.0020)	0.0356 (0.0037)
16	Waist hip ratio	0.21	-0.0098 (0.0022)	0.0000	-0.0019 (0.0021)	0.0122 (0.0012)	0.0121 (0.0017)
	Average across traits		-0.0022 (0.0009)	0.0000	0.0072 (0.0008)	0.0215 (0.0004)	0.0342 (0.0006)

Table S7: Differences between polygenic prediction methods across 16 UK Biobank traits. We report results for P+T, LDpred-inf, P+T-funct-LASSO, LDpred-funct-inf and LDpred-funct. We report the difference between R^2 for each method vs. R^2 for LDpred-inf.

	Method	Average R^2
1	P+T	0.1368
2	LDpred-inf	0.1390
3	P+T-funct-LASSO	0.1475
4	LDpred-funct-inf	0.1606
5	LDpred-funct	0.1739
6	LDpred-inf (typed)	0.1360
7	LDpred-funct-inf (typed)	0.1378
8	LDpred (typed)	0.1117
9	P+T-funct-LASSO-weighted	0.1549
10	P+T-funct-LASSO (5%)	0.1538
11	LDpred-funct-inf (meta31)	0.1560
12	LDpred-funct-inf(baseline)	0.1573
13	LDpred-funct-inf(QCfilters)	0.1606
14	LDpred-funct-inf(UK10K)	0.1601
15	LDpred-funct-inf(UK10K, baseline-LD+LDAK)	0.1600

Table S8: Accuracy of secondary polygenic prediction methods across 16 UK Biobank traits. For each method, we report the average prediction R^2 across 16 UK Biobank traits. Rows 1-5 correspond to the "Average across traits" panel of Figure 2. Rows 6-8 are methods that analyze only genotyped SNPs (601,728 genotyped SNPs after QC). Rows 9-10 are slightly modified versions of P+T-funct-LASSO. Row 11 uses baseline-LD model functional enrichments that were meta-analyzed across 31 traits. Row 12 uses the baseline model, instead of the baseline-LD model. Row 13 restricts the baseline-LD model to the 6,334,603 SNPs that passed QC filters and were used for prediction. Row 14 infers baseline-LD model parameters using UK10K SNPs, instead of 1000 Genomes SNPs. Row 15 uses UK10K SNPs and uses the baseline-LD+LDAK model, instead of the baseline-LD model.

	Trait	LDpred-funct-inf	LDpred-funct-10	LDpred-funct-20	LDpred-funct-50	LDpred-funct-75	LDpred-funct-100
1	Height	0.4019	0.4147	0.4154	0.4153	**0.4161**	0.4152
2	Hair color	0.2472	0.2848	0.2869	**0.2934**	0.2883	0.3035
3	Platelet count	0.2290	0.2448	0.2452	0.2458	**0.2464**	0.2460
4	Bone mineral density	0.2105	0.2213	0.2225	**0.2237**	0.2224	0.2212
5	Red blood cell count	0.1572	0.1669	0.1677	0.1675	0.1681	**0.1682**
6	FEV1-FVC ratio	0.1306	**0.1353**	0.1348	0.1343	0.1336	0.1315
7	Body mass index	0.1501	0.1501	**0.1504**	0.1494	0.1481	0.1473
8	RBC distribution width	0.1429	0.1523	**0.1533**	0.1532	0.1525	0.1508
9	Eosinophil count	0.1336	0.1412	**0.1412**	0.1403	0.1397	0.1386
10	Forced vital capacity	0.1148	**0.1160**	0.1155	0.1145	0.1128	0.1118
11	White blood cell count	0.1249	0.1291	**0.1295**	0.1285	0.1279	0.1262
12	Blood pressure	0.1111	**0.1125**	0.1119	0.1118	0.1108	0.1105
13	Age at menarche	0.1071	0.1118	0.1116	**0.1122**	0.1112	0.1070
14	Tanning ability	0.1234	0.1720	0.1796	0.1858	0.1875	**0.1878**
15	Balding type I	0.1065	0.1217	**0.1235**	0.1220	0.1198	0.1185
16	Waist hip ratio	0.0786	**0.0818**	0.0810	0.0804	0.0798	0.0782
	Average across traits	0.1606	0.1723	0.1731	0.1736	0.1728	0.1726

Table S9: Sensitivity of LDpred-funct results to number of bins used for regularization across 16 UK Biobank traits. We report results with the number of posterior mean causal effect size bins used for regularization (K) set to 10, 20, 50, 75 or 100. LDpred-funct-K denotes each respective value of K. We also report results for LDpred-funct-inf, which is identical to LDpred-funct with K set to 1. For each trait, the column with highest prediction R^2 is denoted in bold font.

			Validation sample size				
	Trait	LDpred-funct-inf	1000	2000	5000	10000	ALL
1	Height	0.4019	0.4007 (0.0052)	0.4171 (0.0026)	0.4162 (0.0019)	0.4154 (0.0016)	0.4167
2	Hair color	0.2472	0.2692 (0.0053)	0.2752 (0.0040)	0.2763 (0.0025)	0.2874 (0.0016)	0.3009
3	Platelet count	0.2290	0.2463 (0.0050)	0.2477 (0.0044)	0.2418 (0.0014)	0.2436 (0.0013)	0.2460
4	Bone mineral density	0.2105	0.2235 (0.0049)	0.2219 (0.0033)	0.2232 (0.0017)	0.2247 (0.0013)	0.2232
5	Red blood cell count	0.1572	0.1579 (0.0047)	0.1743 (0.0039)	0.1667 (0.0016)	0.1672 (0.0011)	0.1673
6	FEV1-FVC ratio	0.1306	0.1373 (0.0055)	0.1348 (0.0026)	0.136 (0.0017)	0.1351 (0.0007)	0.1345
7	Body mass index	0.1501	0.1596 (0.0055)	0.1501 (0.0034)	0.1482 (0.0018)	0.1491 (0.0011)	0.1481
8	RBC distribution width	0.1429	0.1598 (0.0052)	0.1503 (0.0028)	0.1492 (0.0016)	0.1519 (0.0012)	0.1525
9	Eosinophil count	0.1336	0.1492 (0.0052)	0.1439 (0.0042)	0.1402 (0.0014)	0.1406 (0.001)	0.1394
10	Forced vital capacity	0.1148	0.1198 (0.0031)	0.1196 (0.0029)	0.1152 (0.0015)	0.1139 (0.001)	0.1136
11	White blood cell count	0.1249	0.1322 (0.0040)	0.1335 (0.0036)	0.1249 (0.0018)	0.1289 (0.0012)	0.1282
12	Blood pressure	0.1111	0.1170 (0.0033)	0.1114 (0.0020)	0.1112 (0.0013)	0.1100 (0.0009)	0.1111
13	Age at menarche	0.1071	0.1175 (0.0040)	0.1139 (0.0029)	0.1102 (0.0013)	0.1112 (0.0011)	0.1120
14	Tanning ability	0.1234	0.1397 (0.0045)	0.1429 (0.0029)	0.1703 (0.0020)	0.1833 (0.0011)	0.1864
15	Balding type I	0.1065	0.1218 (0.0038)	0.1176 (0.0025)	0.1209 (0.0013)	0.1228 (0.0003)	0.1235
16	Waist hip ratio	0.0786	0.0866 (0.0031)	0.0811 (0.0023)	0.0791 (0.0019)	0.0790 (0.0008)	0.0789
17	Average across traits	0.1606	0.1711	0.1710	0.1706	0.1728	0.1739

Table S10: Sensitivity of LDpred-funct results to number of validation samples across 16 UK Biobank traits. We report results with the number of validation samples set to 1,000, 2,000, 5,000, 10,000 (the number of regularization bins is proportional to the number of validation samples; see Equation 6. Results are averaged across 20 random subsets of each size. ALL denotes results of LDpred-funct using the total number of validation samples (reported in Table S1). We also report results for LDpred-funct-inf, which is equivalent to LDpred-funct in the limit of a very small number of validation samples.

Data Set	Training N	P+T	LDpred-inf	P+T-funct -LASSO	LDpred-funct-inf	LDpred-funct
UK Biobank interim release	113,660	0.2223	0.2305	0.2524	0.2777	0.2926
UK Biobank	408,092	0.3448	0.3677	0.3644	0.3995	0.4132
23andMe	698,430	0.2903	0.2882	0.2985	0.3148	0.3279
Meta-analysis of UK Biobank and 23andMe	1,107,430	0.3710	0.3874	0.3778	0.4193	0.4292
Fixed-effect meta-analysis	1,107,430	0.3687	0.3653	0.3663	0.3965	0.4051

Table S11: Accuracy of 5 prediction methods in height meta-analysis of UK Biobank and 23andMe cohorts. We report results for P+T, LDpred-inf, P+T-funct-LASSO, LDpred-funct-inf and LDpred-funct, for each of 4 training data sets: UK Biobank interim release (113,660 training samples), UK Biobank (408,092 training samples), 23andMe (698,430 training samples) and meta-analysis of UK Biobank and 23andMe (1,107,430 training samples). We also report results for a fixed-effect meta-analysis of UK Biobank and 23andMe.

	Trait	h_g^2	LDpred-funct-inf under different priors: baselineLD (1000G)	baselineLD (UK10K)	baselineLD + LDAK (UK10K)
1	Height	0.579	0.4019	0.4011	0.4018
2	Hair color	0.454	0.2472	0.2501	0.2501
3	Platelet count	0.404	0.2290	0.2294	0.2298
4	Bone mineral density	0.401	0.2105	0.2122	0.2117
5	Red blood cell count	0.324	0.1572	0.1566	0.1544
6	FEV1-FVC ratio	0.313	0.1306	0.1309	0.1323
7	Body mass index	0.308	0.1501	0.1503	0.1502
8	RBC distribution width	0.288	0.1429	0.1432	0.1451
9	Eosinophil count	0.277	0.1336	0.1335	0.1342
10	Forced vital capacity	0.277	0.1148	0.1147	0.1140
11	White blood cell count	0.272	0.1249	0.1246	0.1251
12	Blood pressure	0.271	0.1111	0.1113	0.1136
13	Age at menarche	0.255	0.1071	0.0995	0.0930
14	Tanning ability	0.242	0.1234	0.1206	0.1190
15	Balding type I	0.223	0.1065	0.1040	0.1070
16	Waist hip ratio	0.210	0.0786	0.0793	0.0785

Table S12: Accuracy of LDpred-funct-inf(1000G), LDpred-funct-inf(UK10K) and LDpred-funct-inf(UK10K, baseline-LD+LDAK) across 16 UK Biobank traits. We report results for each trait. Results for Average across traits are reported in Table S8.